Mapping Corpus Callosum Deficits in Autism: An Index of Aberrant Cortical Connectivity

Christine N. Vidal, Rob Nicolson, Timothy J. DeVito, Kiralee M. Hayashi, Jennifer A. Geaga, Dick J. Drost, Peter C. Williamson, Nagalingam Rajakumar, Yihong Sui, Rebecca A. Dutton, Arthur W. Toga, and Paul M. Thompson

Background: *Volumetric studies have reported reductions in the size of the corpus callosum (CC) in autism, but the callosal regions contributing to this deficit have differed among studies. In this study, a computational method was used to detect and map the spatial pattern of CC abnormalities in male patients with autism.*

Methods: *Twenty-four boys with autism (aged 10.0 ± 3.3 years) and 26 control boys (aged 11.0 ± 2.5 years) underwent a magnetic resonance imaging (MRI) scan at 3 Tesla. Total and regional areas of the CC were determined using traditional morphometric methods. Three-dimensional (3D) surface models of the CC were also created from the MRI scans. Statistical maps were created to visualize morphologic variability of the CC and to localize regions of callosal thinning in autism.*

Results: *Traditional morphometric methods detected a significant reduction in the total callosal area and in the anterior third of the CC in patients with autism; however, 3D maps revealed significant reductions in both the splenium and genu of the CC in patients.*

Conclusions: *Statistical maps of the CC revealed callosal deficits in autism with greater precision than traditional morphometric methods. These abnormalities suggest aberrant connections between cortical regions, which is consistent with the hypothesis of abnormal cortical connectivity in autism.*

Key Words: Autism, corpus callosum, imaging, MRI, three-dimensional (3D) maps, white matter

Autism is a developmental disorder characterized by social deficits, impaired communication, and restricted and repetitive patterns of behavior (American Psychiatric Association 2000). There is strong evidence that autism has a neurobiological basis, but the anatomic extent and timing of the biological abnormalities involved in the disorder remain unknown. Consistent with postmortem and head-circumference studies, brain imaging studies suggest that overall brain volumes are increased in children with autism (Nicolson and Szatmari 2003).

Several studies have reported deficits in the size of the corpus callosum (CC) and its subregions, particularly when group differences in brain volume were taken into consideration. Reduced total cross-sectional callosal areas have been reported in several studies (Boger-Megiddo et al 2003; Egaas et al 1995; Manes et al 1999). When the subregions of the CC have been examined, however, the results have been inconsistent. Several groups have reported reductions in the size of the body and posterior subregions of the CC in autistic patients (Egaas et al 1995; Haas et al 1996; Piven et al 1997; Saitoh et al 1995), whereas others have only found significant differences in the anterior regions (Hardan et al 2000) or in the body of the CC (Manes et al 1999). Recently, two studies using voxel-based morphometry have reported reductions in the area of the splenium and isthmus (Waiter et al 2005) and the genu, rostrum, and splenium of the CC (Chung et al 2004) in patients with autism. To date, only two studies (Elia et al 2000; Herbert et al 2004) have failed to find any differences in CC size between patients and control subjects, although it should be noted that neither of these studies examined callosal differences after controlling for group differences in brain size.

Consequently, although magnetic resonance imaging (MRI) studies to date have generally reported reductions in callosal size in patients with autism, the regions that differ between patients and control subjects have not been consistent. This inconsistency may be due, at least in part, to factors such as sample size, subject age and gender, specific diagnosis (i.e., autism, Asperger syndrome, or pervasive developmental disorder not otherwise specified), and the presence or absence of mental retardation. Additionally, the neuroanatomic definition of the CC may have contributed to the inconsistency seen in studies of the CC in autism. To examine regional differences in callosal size, all of the previous studies apart from the two using voxel-based morphometry (Chung et al 2004; Waiter et al 2005) subdivided the CC using the scheme suggested by Witelson (1989). Although this method has been widely used, it arbitrarily divides the CC into several regions according to maximal length and thus could be biased by local variability in callosal shape. Furthermore, the Witelson partition may be less likely to capture subtle regional group differences in anatomy, particularly if these differences are not spatially uniform across a region.

Recently, however, computational mapping methods have been developed to examine CC structure. The use of surface mesh models and statistical maps permits the examination of highly localized group differences in callosal size and shape while preserving subtle variability patterns within groups (Thompson et al 2000, 2003). Although this approach is complementary to voxel-based methods that assess differences in tissue types at each voxel of stereotaxic space, the shape-modeling approach works by averaging the geometry of the anatomic models rather than comparing segmented images. Previous studies using these computational methods have detected regional alterations of callosal morphology in schizophrenia (Narr et al 2002).

From the Laboratory of Neuro Imaging (CNV, KMH, JAG, YS, RAD, AWT, PMT), Brain Mapping Division, Department of Neurology, UCLA School of Medicine, Los Angeles, California; and Departments of Psychiatry (RN, PCW, NR) and Medical Biophysics (TD, DJD), University of Western Ontario, London, Ontario, Canada.

Address reprint requests to Dr. Paul Thompson, Laboratory of Neuro Imaging, Department of Neurology, UCLA School of Medicine, 635 Charles E. Young Drive South, Suite 225E, Los Angeles, CA 90095-7332; E-mail: thompson@loni.ucla.edu.

Received February 4, 2005; revised November 1, 2005; accepted November 3, 2005.

0006-3223/06/$32.00
doi:10.1016/j.biopsych.2005.11.011

Geometric anatomic models and statistical maps have not previously been employed in studies of callosal abnormalities in autism. In this study, computational mapping methods were used to detect and visualize the spatial patterns of CC abnormalities in children and adolescents with autism. A novel measurement of CC thickness (the distance from a medial line) was combined with a shape-averaging technique to create models of the CC that could be used to visualize differences in CC size and shape between groups. Furthermore, CC size was statistically compared across models using parametric curves, a method which has not been previously applied to studies of the CC in autism. We hypothesized that we would detect specific callosal regions with thinning in children with autism, revealing the scope and extent of the callosal abnormalities in the disorder.

Methods and Materials

Subjects

Twenty-four boys with autism (aged 10.0 ± 3.3 years; range 6–16 years) participated in this study. The diagnosis was made using the Autism Diagnostic Interview—Revised (ADI-R; Lord et al 1994), the Autism Diagnostic Observation Schedule (ADOS-R; Lord et al 2000), and by clinical observation. All patients met DSM-IV-TR criteria for autism (American Psychiatric Association 2000) as well as ADI-R and ADOS algorithm criteria. Patients were also assessed using the Wechsler Intelligence Scale for Children, 3rd Edition (WISC-III) or the Leiter International Performance Scale. Socioeconomic status was determined for each patient (Hollingshead 1975). Patients with a nonverbal IQ < 70 were excluded from participation. All patients had a physical examination before participation in this study, and subjects with a seizure disorder or other neurologic condition or a cytogenetic abnormality or genetic syndrome (such as fragile X syndrome) were also excluded from participation. At the time of the scan, eight patients were medication-naïve, and four others had discontinued their previous medications before the scan. Among the remainder, five were being treated with dopamine antagonists, eight were taking stimulants, four were receiving selective serotonin reuptake inhibitors, and one was being treated with a cholinesterase inhibitor.

Twenty-six healthy boys (aged 11.0 ± 2.5 years; range 6–16 years), drawn from the local community through advertisement and word of mouth, participated as control subjects in this study. They were assessed with the Schedule for Affective Disorders and Schizophrenia—Childhood Version (K-SADS; Kaufman et al 1997) to ensure that none had a major psychiatric disorder. Additionally, none had a personal history of neurologic disorders or learning disorders or a family history of autism, mental retardation, language disorders, or learning disorders. Control subjects were also assessed with the WISC-III or the Wechsler Abbreviated Scale of Intelligence, and a full-scale IQ < 70 was exclusionary. Socioeconomic status was also determined for each control subject (Hollingshead 1975).

This study was approved by the Health Sciences Research Ethics Board at the University of Western Ontario. The parents or legal guardians of all subjects provided written consent for participation in this study, and the subjects provided written assent.

Magnetic Resonance Imaging

All subjects were scanned on a 3-Tesla head-only scanner (IMRIS, Winnipeg, Canada) with a quadrature head coil. To facilitate completion of their scans, 16 patients with autism received sedation with oral midazolam.

Standard T_1-weighted localizer images were acquired initially. Images used for volumetric analysis were then acquired using a T_1-weighted three-dimensional (3D) MP-RAGE (Magnetization Prepared Rapid Gradient Echo) sequence (inversion time = 200 msec, repetition time = 11 msec, echo time = 5 msec, flip angle = 12°, total scan time: 8 min) with 1.2-mm isotropic voxels.

Image Processing and Analysis

Each brain volume was corrected for radiofrequency field inhomogeneities (Sled et al 1998) and resliced into a standard orientation. Twenty standard anatomic landmarks were identified in all three planes by a trained operator (CV) and matched with a set of corresponding point locations defined on the ICBM53 stereotaxic space (Mazziotta et al 2001). These landmarks were used to compute a three-translation and three-rotation rigid-body linear transformation for each brain volume to align it to the standardized coordinate system of the ICBM53 average brain. Each brain volume was reoriented to correct for head alignment and resampled to 1.0-mm isotropic voxels using trilinear interpolation and a six-parameter Procrustes fit.

Corpus Callosum Modeling

One rater (CV), blind to age and diagnosis, repeatedly traced the CC (allowing for the quantification of reliability) in each magnified brain volume by following white matter tissue boundaries with a mouse-driven cursor. The CC was modeled as a single two-dimensional curve in the midsagittal plane.

Area Measurement

To apply traditional regional analyses, the callosal renderings were reoriented and divided using a modification of the Witelson partitioning scheme (Clarke and Zaidel 1994; Witelson 1989) into five discrete partitions representing the 1) splenium, 2) isthmus, 3) posterior midbody, 4) anterior midbody, and 5) anterior third (see Figure 1A). Area measures were computed in mm^2 for each callosal segment. For each section of the CC and the total area, intrarater reliability was high (all intraclass correlation coefficients > .90), and previous studies in our lab using this methodology have also demonstrated high interrater reliability (intraclass correlation coefficients > .95; Narr et al 2002).

Medial Curve Construction and Thickness Measurement

After converting the top and bottom of the CC into a set of uniformly spaced points, a medial line was calculated as an average curve between the superior and inferior CC boundaries, as seen in Figure 1A. The two points where the superior and inferior boundaries connected were defined as the most posterior point of the splenium and the most anterior point of the anterior third of the CC (see Figure 1A). At each point on the upper and lower traces, the distance to the medial line was computed and plotted on the upper and lower trace (Figure 1B). This measure of thickness at each CC surface point was retained for averaging and comparison across subjects within each group (Figure 1C).

Anatomic Shape Averaging

Three-dimensional maps were also created to emphasize average difference between groups in callosal shape, visualizing the regions with statistical differences (see Figure 2D). Anatomic mesh modeling methods were used to match equivalent callosal surface points, obtained from manual tracings, across subjects

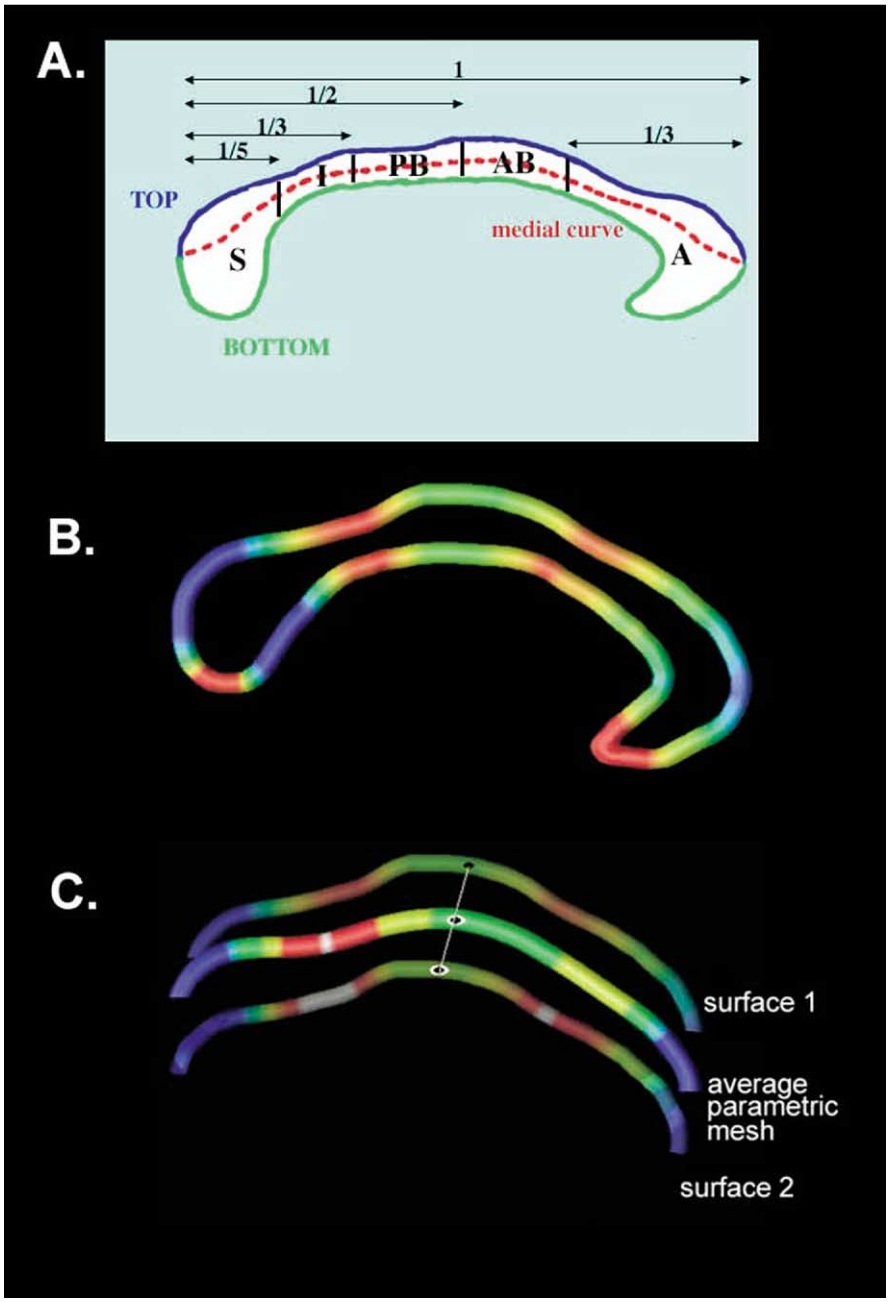

Figure 1. (A) Modified Witelson scheme for partitioning the corpus callosum (CC; Clarke and Zaidel 1994). Creation of medial line, measurement of callosal thickness, and anatomic surface averaging. The CC outlines, created from callosal tracings, were split into top (blue) and bottom (green) surfaces and a medial line equidistant to each surface was computed. **(B)** The distances between the medial line and the top and bottom surfaces were calculated. Points representing boundaries of the corpus callosum were digitized to render each set of callosal points uniform. **(C)** Points from each surface boundary were averaged to generate an average callosal boundary for each subject group, with average measures of thickness plotted on it in color. All results in this figure were computed without using age as a variate. A, anterior third; AB, anterior midbody; I, isthmus; PB, posterior midbody; S, splenium.

and groups. To match the digitized points representing the callosal surface traces in each brain volume, manually derived contours, from the midsagittal slice and from the 4 adjacent slices either side of midline, were made spatially uniform by modeling them as a 3D parametric surface mesh. This resulted in a 3D model of the CC that extended 4 mm into each hemisphere. The spatial frequency of digitized points making up the callosal surface traces was equalized within and across brain slices. These procedures allow measurements to be made at corresponding surface locations in each subject that may then be compared statistically. The matching procedures also allow the averaging of callosal surface morphology across all individuals belonging to a group and record the amount of variation between corresponding surface points relative to the group averages.

Statistical Maps and Permutation Tests

Age, race, socioeconomic status, handedness, height, and intelligence were compared between the two groups using *t* tests or chi-square analyses.

Thickness measures allow greater localization of deficits but may be less sensitive to differences in anterior–posterior length of the CC. As a result, volumetric or regional cross-sectional area measures may in some cases be more sensitive than thickness maps for detecting group differences and vice versa. To compare both methods, we used both traditional volumetric methods and statistical maps.

Using the modified Witelson partition (Figure 1A), traditional anatomic measures, both global and regional, were compared between groups using analysis of variance (ANOVA). Age did

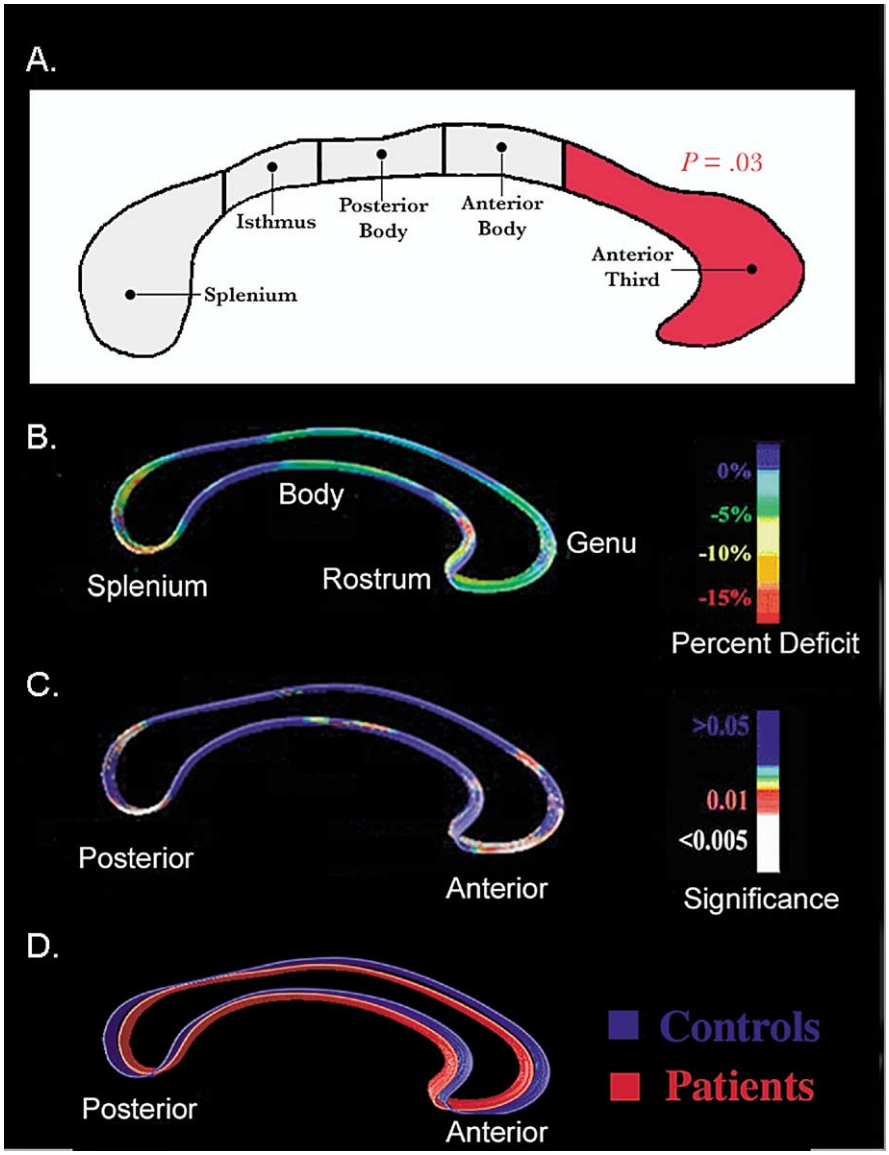

Figure 2. Scaled corpus callosum (CC) maps comparing patients with autism and control subjects. **(A)** Modified Witelson partitioning scheme. The anterior third of the CC showed a significant area reduction in autism. **(B)** Reduction of CC thickness in autism, expressed as a percentage relative to control subjects. **(C)** Significance of mean local CC thinning in autistic subjects relative to control subjects. **(D)** Shape differences in CC between patients and control subjects.

not differ significantly between the groups, but the age range in this study was wide (6–16 years). As such, we also covaried the analyses of morphometric data for age to reduce error variance and increase statistical power.

Variations in CC shape and thickness, within each subject group, were assessed at each CC surface point. The thickness maps were averaged across subjects within each group (across corresponding points defined by the uniform parametric mesh), and group differences were assessed at each surface location by *t* tests. Mean group differences in callosal thickness were plotted as a percentage reduction in local thickness (Figure 2B), and regions exhibiting statistically significant differences in thickness (with $p < .05$) were coded in color on the surface meshes (Figure 2C). Permutation testing of the shape statistics was used to assess the significance of the overall differences in thickness. This accounts for the spatial autocorrelation of the residuals of the statistical model while adjusting for the multiple comparisons implicit in conducting multiple statistical tests at each point on a surface (Nichols and Holmes 2002).

Brain Size Correction

For statistical mapping of CC surface parameters, image volumes and the CC contours associated with each image volume were generated in stereotaxic space, which adjusts for differences in brain size. Uncertainty exists, however, as to whether brain size corrections increase or decrease error variance for regions of interest comparisons (Mathalon et al 1993). To allow for either possibility, we built the same anatomic maps and performed the same comparisons using raw ("descaled") CC volumes. These were derived by dividing each CC volume by the scaling factor used to transform it to the ICBM53 average brain. To descale the 3D maps created previously, the inverse of the global scaling transformation matrix (with nine parameters) was applied to the CC traces. The least squares rigid transform with six parameters (without scaling) was then applied to the resulting CC traces to align them rigidly with the ICBM53 average brain data set. Maps of group differences were created both before and after adjusting for any individual and group differences in brain size.

Table 1. Demographic and Clinical Characteristics of Patients with Autism and Control Subjects

Demographic Measure	Autism ($n = 24$)	Control ($n = 26$)	Test Statistic	*df*	*p* Value
Age (years)	10.0 ± 3.3	11.0 ± 2.5	t = 1.4	48	.2
Race (# Caucasian)	23/24	26/26	$\chi^2 = 1.1$	1	.3
Socioeconomic Status	55.7 ± 23.6	49.8 ± 17.2	t = 1.0	46	.3
Height (cm)	143.9 ± 19.5	147.4 ± 14.9	t = .7	44	.5
Head Circumference (cm)	55.4 ± 2.6	54.9 ± 1.7	t = .9	48	.4
Handedness (right:left)	18:6	26:0	$\chi^2 = 7.4$	1	.007
Verbal IQ	92.9 ± 13.3	105.4 ± 11.2	t = 3.3	41	.002
Nonverbal IQ	99.1 ± 14.0	104.1 ± 14.0	t = 1.2	46	.2
Full-Scale IQ Score	95.9 ± 11.5	104.8 ± 11.7	t = 2.5	41	.02

All continuous data presented as mean ± SD.

Results

Subjects

The groups did not differ significantly in terms of age, socioeconomic status, race, or height (see Table 1), although there was a significantly greater proportion of left-handed subjects in the patient group. Although there was no significant difference in nonverbal IQ between the two groups, patients did have a significantly lower verbal and full-scale IQ.

Traditional CC Measurements

Using the descaled (native space) images, the groups did not differ in total callosal area or in any of the callosal subsections (see Table 2). When total brain size was controlled for through scaling, however, the total CC area ($p = .048$) was significantly smaller in the patients with autism. Additionally, patients had a significant reduction in the area of the anterior third of the CC ($p = .03$; see Figure 2A) and a nonsignificant trend for a reduction in the size of the posterior midbody ($p = .06$). As seen in Table 2, the pattern of results and significant differences was essentially identical when age was used as a covariate. Additionally, when total brain volume was used as a covariate to control for group differences in brain volume rather than scaling, the pattern of results and significant differences was identical to that seen when scaling was used to control for differences in brain volume.

Based on reports of abnormalities of handedness and cerebral lateralization in autism (e.g., Dawson 1988), the use of handedness as a covariate in our analyses of the morphometric data did not seem warranted as differences in handedness may in part reflect the neurobiologic abnormalities underlying autism. Nevertheless, we explored the data from the modified Witelson partitioning of the CC using handedness as a covariate and also restricting analyses to right-handed patients and found no change either in the pattern or statistical significance of the results.

Computational Mapping

Permutation tests on the descaled (native space) group average map of the CC revealed a significant reduction in thickness in the splenium in patients with autism ($p = .02$); however, when total brain size was controlled for through the use of the scaled maps, the group average computational map of the CC showed a reduction in thickness in three areas: the splenium, body, and genu (see Figure 2B and 2C). Permutation tests run on these specific regions of interest showed that the splenium ($p = .0006$) and the genu ($p = .006$) were significantly reduced in patients

Table 2. Corpus Callosum Measures in Subjects with Autism and Healthy Control Subjects

			ANOVA		ANCOVA[b]	
Corpus Callosum Measure[a]	Autism ($n = 24$)	Control ($n = 26$)	*F*	*p*	*F*	*p*
Total Brain Volume	1581.9 ± 132.1	1569.0 ± 97.8	0.2	0.7	0.5	0.5
Raw (Descaled) Measures						
Total Area	468.2 ± 103.8	499.7 ± 70.8	1.6	.2	2.2	.1
Witelson Partition Areas						
Splenium	121.2 ± 37.7	128.6 ± 17.0	.8	.4	.9	.3
Isthmus	42.3 ± 12.0	42.9 ± 8.7	.4	.8	.1	.8
Posterior midbody	46.8 ± 10.8	50.8 ± 9.5	1.9	.2	1.8	.2
Anterior midbody	57.5 ± 12.0	59.5 ± 10.6	.4	.5	.7	.4
Anterior third	195.5 ± 40.6	212.7 ± 37.1	2.4	.1	3.9	.05
Scaled Measures						
Total Area	612.8 ± 131.3	674.8 ± 80.1	4.1	.05	6.2	.02
Witelson Partition Areas						
Splenium	158.4 ± 46.4	174.0 ± 22.2	2.4	.1	3.0	.09
Isthmus	55.2 ± 15.0	57.9 ± 11.1	.5	.5	.8	.4
Posterior midbody	61.2 ± 14.4	68.5 ± 11.9	3.8	.06	4.0	.05
Anterior midbody	75.2 ± 15.5	80.3 ± 12.8	1.6	.2	2.6	.1
Anterior third	256.2 ± 52.9	286.8 ± 41.5	5.2	.03	9.3	.004

All data presented as mean ± SD. ANCOVA, analysis of covariance; ANOVA, analysis of variance.
[a]All area measurements are given in mm^2, and total brain volume is in cm^3; $df = 1,48$ for all ANOVA and 1,47 for all ANCOVA.
[b]ANCOVA completed using age as covariate.

with autism, although the permutation test on the body of the CC did not show a significant group difference. Overlaid shapes of the CC in normal and autistic subjects showed differences in anatomic shape between the two groups, with patients having a reduced anterior–posterior length and reduced arching of the callosal midbody (see Figure 2C).

Discussion

To our knowledge, this is the first study to use computational mapping methods to investigate CC abnormalities in autism. Although traditional morphometric methods revealed a significant reduction in the total area of the CC and of the anterior CC, computational mapping revealed more precise areas of significant thinning in both the genu and in the splenium.

Other groups have reported a reduction in the total area of the CC (Boger-Megiddo et al 2003; Egaas et al 1995; Manes et al 1999), but subregional findings have been mixed. Although reductions of the anterior, midbody, or posterior CC have been noted in various studies, only one (Chung et al 2004) has reported reductions both anteriorly and posteriorly. In our study, traditional morphometric methods detected differences only in the anterior third of the CC, whereas the use of computational mapping resulted in much more specific localization of the abnormalities in both the genu and the splenium. The lower power of volumetric measures may explain why studies using them, both here and elsewhere, have typically not found differences, both anteriorly and posteriorly in patients with autism. If deficit patterns are not spatially uniform, computational shape mapping may provide increased power for group discrimination relative to volumetric measures and thus a greater likelihood of detecting group differences (Thompson et al 2003). When effects are highly localized, maps are likely to detect deficits that volumetric measures may miss, and diffuse effects are likely to be identified with comparable power using either approach. Because no formal anatomic subdivision is necessary when the surface meshes are compared, the mapping approach is also suitable for mapping deficit regions that may not necessarily coincide neatly with the Witelson partitioning boundaries.

The greater spatial localization of regional reductions in CC size permits a greater insight into the cortical regions potentially related to the callosal abnormalities seen in patients with autism. In addition to previous reports of morphometric abnormalities of the anterior corpus callosum (Hardan et al 2000; Chung et al 2004), a study using diffusion tensor imaging also noted abnormalities of fractional anisotropy in the anterior corpus callosum (Barnea-Goraly et al 2004). In our study, the region with a reduction in thickness within the genu occurs where fibers from the orbitofrontal cortex cross the CC (Barbas and Pandya 1985). The orbitofrontal cortex appears to be important in appropriately interpreting social and emotional cues (Mah et al 2004), and has been implicated in the neuroanatomy of "theory of mind" (Sabbagh 2004), that is, the ability to make hypotheses about another person's mental state. Although abnormalities of orbitofrontal white matter have not been reported in neuroimaging studies of autism, Chung and colleagues (2005) did note a reduction in cortical thickness in the right orbitofrontal cortex. The region of reduction in thickness in the midbody corresponds to the location where fibers from the primary and secondary somatosensory cortex cross the CC, and a recent neuroimaging study using voxel-based morphometry noted a decrease in white matter volume in the primary somatosensory area (Waiter et al 2005). The reductions in thickness in the splenium correspond to regions where fibers from the parahippocampal gyrus and the visual association cortex cross the midline (Rockland and Pandya 1986). Waiter and colleagues (2004) noted a localized increase in the volume of the left parahippocampal gyrus in patients with autism, whereas a later study by the same group (Waiter et al 2005) reported a reduction in the white matter volume of the left visual association area.

Potential biological processes leading to a reduction in CC size given reports of exaggerated postnatal growth in head size and later brain volume enlargement in autism (reviewed in Nicolson and Szatmari, 2003) are of interest. It has been reported that callosal size does not increase in proportion to brain size (Jancke et al 1999), suggesting that the degree of interhemispheric connectivity decreases with increasing brain size, perhaps due to the increasing time constraints of transcallosal conduction delay (Ringo 1991). The increased brain size reported in autism, in conjunction with the disproportionately reduced CC size, may place increased constraints on transcallosal connectivity and, as a result, an increased emphasis on interhemispheric connectivity. Consistent with this hypothesis, Herbert and colleagues (2004) reported that the increase in white matter volume in patients with autism was associated with an increase in superficial or radiate white matter, whereas deeper white matter did not differ from that of control subjects. Thus, intrahemispheric corticocortical fibers may be increased in autism whereas interhemispheric fibers are not, resulting in a disproportionate increase in brain volume in comparison to callosal size. Although the developmental factors leading to localized reductions in callosal size in autism are unknown, it is possible that growth of different CC regions is governed by different processes. For example, different mechanisms may control development of the CC across the rostrocaudal and dorsoventral axes (Richards et al 2004), and perturbations of these mechanisms may lead to abnormalities in the growth of one or more sections while sparing others.

Based on studies indicating a positive correlation between midsagittal CC area and the total number of fibers traversing this commissure (Aboitiz et al 1992), the reduction in regional and total CC area seen in patients with autism suggests a reduction in the number of axonal fibers traversing the CC. This would suggest abnormalities of cortical connectivity, and it has been proposed that autism is associated with a reduction in functioning of integrative circuitry that results in deficits of cortical connectivity and integration of information (Belmonte et al 2004). Abnormalities of connectivity could lead to a disruption of any psychologic or neurologic function that is dependent on the coordination or integration of different brain regions, and in fact, neuropsychologic impairments in autism are most apparent in those domains with the greatest demands on integrative processing (Minshew et al 2002). Although the finding of a reduction in size of the CC is consistent with the hypothesis of reduced cortical connectivity in autism, conclusions about the cause and significance of the reduction in CC size in autism must be made cautiously, particularly because the relationship between size of the CC and the number of callosal fibers is not entirely clear (Lamantia and Rakic 1990).

The results of this study need to be interpreted cautiously because of several limitations including the small sample size. The lack of female subjects limits the conclusions that can be drawn about female patients with autism. At the same time, given the known gender differences in prevalence and severity of autism (Yeargen-Alsop et al 2003) and in brain development

(Giedd and Lenroot 2005), the inclusion of only male subjects in this study may have highlighted group differences by removing gender variables that affect neurodevelopment. A number of patients in the study were taking psychotropic medication, which could potentially have influenced the results, although this seems unlikely given that other patient groups taking similar medications to those used in patients with autism have not shown abnormalities of the corpus callosum (Kumra et al 2000). Finally, a minor limitation of the study is that some manual interaction with the images is required to trace the CC, whereas some other methods, such as voxel-based morphometry, are completely automated. If automated CC segmentation methods become as reliable as manual tracing, these shape analysis methods may be efficiently extended to larger samples.

In conclusion, patients with autism had a reduction in the total area of the CC. A novel anatomical mapping strategy was used to detect and visualize highly localized patterns of callosal thinning in children with autism, with the greatest abnormalities being noted in the genu and splenium. Shape and computational mapping can provide increased power for group discrimination relative to volumetric measures, especially when deficits are localized, and, as such, these maps may reveal the spatial pattern of CC deficits in autism with greater precision and statistical power than traditional volumetric methods. Future studies with related, nonautistic groups of patients, particularly patients with language disorders, are needed to determine the diagnostic specificity of the callosal abnormalities reported here.

This work was funded by grants from the National Institute for Biomedical Imaging and Bioengineering, the National Center for Research Resources, and the National Institute on Aging (to PT, Grant Nos. R21 EB01651, R21 RR019771, and P50 AG016570). Additional support was provided by the Child and Parent Resource Institute and grants from the London Health Sciences Foundation, the Ontario Mental Health Foundation, and the Hospital for Sick Children Foundation (RN), and by a Human Brain Project grant to the International Consortium for Brain Mapping, funded jointly by NIMH and NIDA (Grant Nos. P20 MH/DA52176, P41 RR13642, and P20 MH65166 to AWT). This work was presented at the Annual Meeting of the International Society for Magnetic Resonance in Medicine, Toronto, 2003.

Aboitiz F, Scheibel AB, Fisher RS, Zaidel E (1992): Fiber composition of the human corpus callosum. *Brain Res* 598:143–153.

American Psychiatric Association (2000): *Diagnostic and Statistical Manual of Mental Disorders,* 4th ed., text revision. Washington, DC: American Psychiatric Association.

Barbas H, Pandya DN (1985): Topography of commissural connections of the prefrontal cortex in the rhesus monkey. *Exp Brain Res* 55:187–191.

Barnea-Goraly N, Kwon H, Menon V, Eliez S, Lotspeich L, Reiss AL (2004): White matter structure in autism: Preliminary evidence from diffusion tensor imaging. *Biol Psychiatry* 55:323–326.

Belmonte MK, Allen G, Beckel-Mitchener A, Boulanger LM, Carper RA, Webb SJ (2004): Autism and abnormal development of brain connectivity. *J Neurosci* 24:9228–9231.

Boger-Megiddo I, Shaw DW, Friedman SD (2003): Cerebral volumetrics and corpus callosum correlations in autism. Presented at the Annual Meeting of the International Society for Magnetic Resonance Imaging in Medicine, Toronto.

Chung MK, Dalton KM, Alexander AL, Davidson RJ (2004): Less white matter concentration in autism: 2D voxel-based morphometry. *Neuroimage* 23: 242–251.

Chung MK, Robbins SM, Dalton KM, Davidson RJ, Alexander AL, Evans AC (2005): Cortical thickness analysis in autism with heat kernel smoothing. *Neuroimage* 25:1256–1265.

Clarke JM, Zaidel E (1994): Anatomical–behavioral relationships: Corpus callosum morphometry and hemispheric specialization. *Behav Brain Res* 64:185–202.

Dawson G (1988): Cerebral lateralization in autism: Clues to its role in language and affective development. In: Molfese DL, Segalowitz SJ, editors. *Brain Lateralization in Children: Developmental Implications*. New York: Guilford Press.

Egaas B, Courchesne E, Saitoh O (1995): Reduced size of corpus callosum in autism. *Arch Neurol* 52:794–801.

Elia M, Ferri R, Musumeci SA, Panerai S, Bottitta M, Scuderi C (2000): Clinical correlates of brain morphometric features of subjects with low-functioning autistic disorder. *J Child Neurol* 15:504–508.

Giedd J, Lenroot R (2005): Sexual dimorphism of brain developmental trajectories during childhood and adolescence. Annual Meeting of the Organization for Human Brain Mapping, Toronto.

Haas RH, Townsend J, Courchesne E, Lincoln AJ, Schreibman L, Yeung-Courchesne R (1996): Neurologic abnormalities in infantile autism. *J Child Neurol* 11:84–92.

Hardan AY, Minshew NJ, Keshavan MS (2000): Corpus callosum size in autism. *Neurology* 55:1033–1036.

Herbert MR, Ziegler DA, Makris N, Filipek PA, Kemper TL, Normandin JJ, et al (2004): Localization of white matter volume increase in autism and developmental language disorder. *Ann Neurol* 55:530–540.

Hollingshead AB (1975): *Four Factor Analysis of Social Status*. New Haven, CT: Yale University Department of Sociology.

Jancke L, Preis S, Steinmetz H (1999): The relation between forebrain volume and midsagittal size of the corpus callosum in children. *Neuroreport* 10:2981–1985.

Kaufman J, Birmaher B, Brent D, Rao U, Flynn C, Moreci P, et al (1997): Schedule for Affective Disorders and Schizophrenia for School-Age Children-Present and Lifetime Version (K-SADS-PL): Initial reliability and validity data. *J Am Acad Child Adolesc Psychiatry* 36:980–988.

Kumra S, Giedd JN, Vaituzis AC, Jacobsen LK, McKenna K, Bedwell J, et al (2000): Childhood-onset psychotic disorders: Magnetic resonance imaging of volumetric differences in brain structure. *Am J Psychiatry* 157: 1467–1474.

Lamantia AS, Rakic P (1990): Cytological and quantitative characteristics of four cerebral commissures in the rhesus monkey. *J Comp Neurol* 291: 520–537.

Lord C, Risi S, Lambrecht L, Cook EH Jr, Leventhal BL, DiLavore PC, et al (2000): The autism diagnostic observation schedule-generic: A standard measure of social and communication deficits associated with the spectrum of autism. *J Autism Dev Disord* 30:205–223.

Lord C, Rutter M, Le Couteur A (1994): Autism Diagnostic Interview—Revised: A revised version of a diagnostic interview for caregivers of individuals with possible pervasive developmental disorders. *J Autism Dev Disord* 24:659–685.

Mah L, Arnold MC, Grafman J (2004): Impairment of social perception associated with lesions of the prefrontal cortex. *Am J Psychiatry* 161:1247–1255.

Manes F, Piven J, Vrancic D, Nanclares V, Plebst C, Starkstein SE (1999): An MRI study of the corpus callosum and cerebellum in mentally retarded autistic individuals. *J Neuropsychiatry Clin Neurosci* 11:470–474.

Mathalon DH, Sullivan EV, Rawles JM, Pfefferbaum A (1993): Correction for head size in brain-imaging measurements. *Psychiatry Res* 50:121–139.

Mazziotta J, Toga A, Evans A, Fox P, Lancaster J, Zilles K, et al (2001): A probabilistic atlas and reference system for the human brain: International Consortium for Brain Mapping (ICBM). *Philos Trans R Soc Lond B Biol Sci* 356:1293–1322.

Minshew NJ, Sweeney J, Luna B (2002): Autism as a selective disorder of complex information processing and underdevelopment of neocortical systems. *Mol Psychiatry* 7(suppl 2):S14–15.

Narr KL, Cannon TD, Woods RP, Thompson PM, Kim S, Asunction D, et al (2002): Genetic contributions to altered callosal morphology in schizophrenia. *J Neurosci* 22:3720–3729.

Nichols TE, Holmes AP (2002): Nonparametric permutation tests for functional neuroimaging: A primer with examples. *Hum Brain Mapp* 15: 1–25.

Nicolson R, Szatmari P (2003): Genetic and neurodevelopmental influences in autistic disorder. *Can J Psychiatry* 48:526–537.

Piven J, Bailey J, Ranson BJ, Arndt S (1997): An MRI study of the corpus callosum in autism. *Am J Psychiatry* 154:1051–1056.

Richards LJ, Plachez C, Ren T (2004): Mechanisms regulating the development of the corpus callosum and its agenesis in mouse and human. *Clin Genet* 66:276–289.

Ringo JL (1991): Neuronal interconnection as a function of brain size. *Brain Behav Evol* 38:1–6.

Rockland KS, Pandya DN (1986): Topography of occipital lobe commissural connections in the rhesus monkey. *Brain Res* 365:174–178.

Sabbagh MA (2004): Understanding orbitofrontal contributions to theory-of-mind reasoning: implications for autism. *Brain Cogn* 55:209–219.

Saitoh O, Courchesne E, Egaas B, Lincoln AJ, Schreibman L (1995): Cross-sectional area of the posterior hippocampus in autistic patients with cerebellar and corpus callosum abnormalities. *Neurology* 45:317–324.

Sled JG, Zijdenbos AP, Evans AC (1998): A nonparametric method for automatic correction of intensity nonuniformity in MRI data. *IEEE Trans Med Imaging* 17:87–97.

Thompson PM, Giedd JN, Woods RP, MacDonald D, Evans AC, Toga AW (2000): Growth patterns in the developing brain detected by using continuum mechanical tensor maps. *Nature* 404:190–193.

Thompson PM, Narr KL, Blanton RE, Toga AW (2003): Mapping structural alterations of the corpus callosum during brain development and degeneration. In: Iacoboni M, Zaidel E, editor. *The Parallel Brain*. Cambridge, MA: MIT Press.

Waiter GD, Williams JH, Murray AD, Gilchrist A, Perrett DI, Whiten A (2004): A voxel-based investigation of brain structure in male adolescents with autism spectrum disorder. *Neuroimage* 22:619–625.

Waiter GD, Williams JH, Murray AD, Gilchrist A, Perrett DI, Whiten A (2005): Structural white matter deficits in high-functioning individuals with autistic spectrum disorder: A voxel-based investigation. *Neuroimage* 24: 455–461.

Witelson SF (1989): Hand and sex differences in the isthmus and genu of the human corpus callosum. A postmortem morphological study. *Brain* 112: 799–835.

Yeargin-Allsop M, Rice C, Karapurkar T, Doernberg N, Boyle C, Murphy C (2003): Prevalence of autism in a US metropolitan area. *JAMA* 289:48–55.